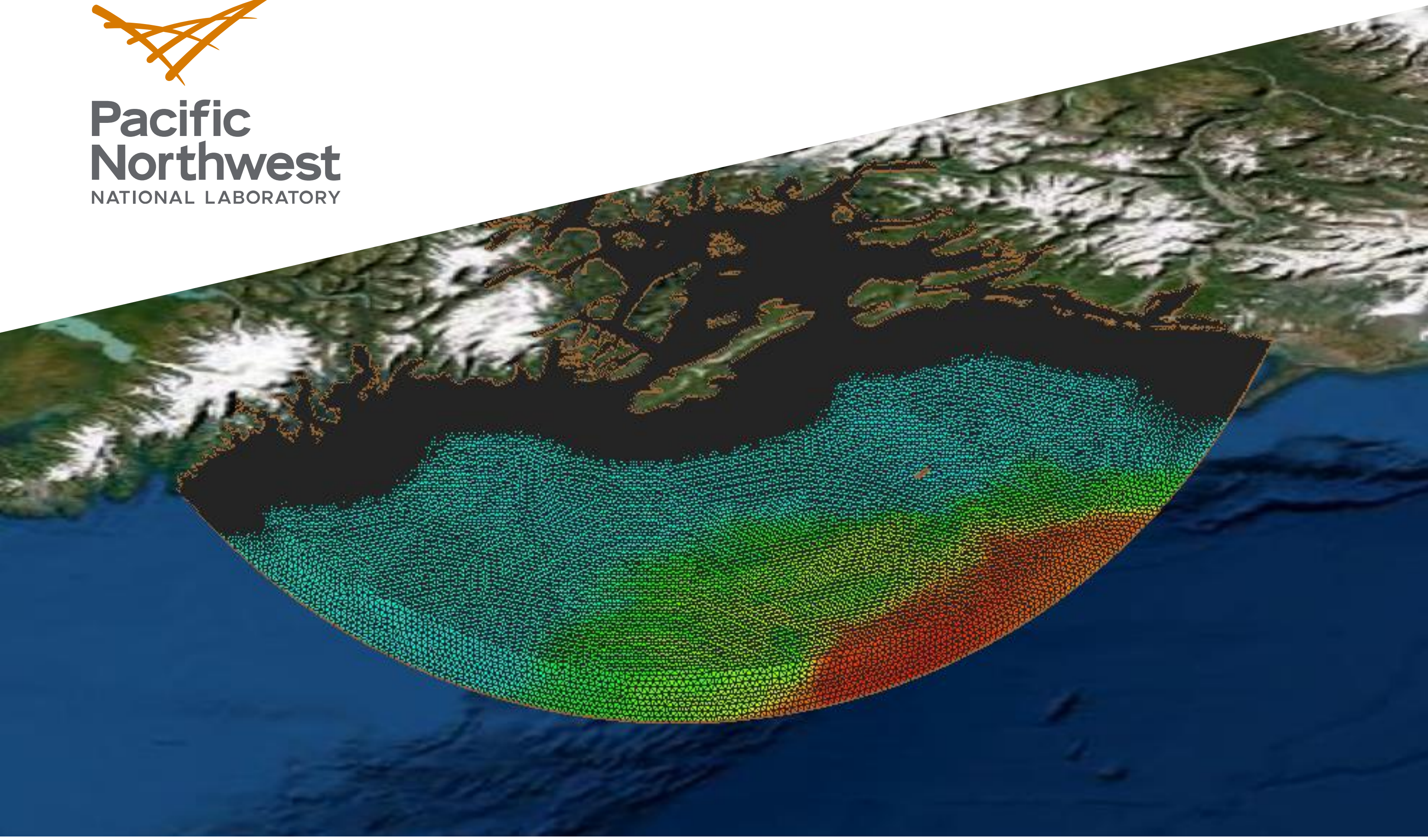

PNNL- 30235

Sea-Ice Effects on the Alaskan Wave Climate

August 2020

Z Yang
R Branch
G Garcia Medina
T Wang

Prepared for the U.S. Department of Energy
under Contract DE-AC05-76RL01830

PACIFIC NORTHWEST NATIONAL LABORATORY
operated by
BATTELLE
for the
UNITED STATES DEPARTMENT OF ENERGY
under Contract DE-AC05-76RL01830

Printed in the United States of America

**Available to DOE and DOE contractors from the
Office of Scientific and Technical Information,
P.O. Box 62, Oak Ridge, TN 37831-0062;
ph: (865) 576-8401
fax: (865) 576-5728
email: reports@adonis.osti.gov**

**Available to the public from the National Technical Information Service
5301 Shawnee Rd., Alexandria, VA 22312
ph: (800) 553-NTIS (6847)
email: orders@ntis.gov <https://www.ntis.gov/about>
Online ordering: http://www.ntis.gov**

PNNL- 30235

Sea-Ice Effects on the Alaskan Wave Climate

August 2020

Z Yang
R Branch
G Garcia Medina
T Wang

Prepared for
the U.S. Department of Energy
under Contract DE-AC05-76RL01830

Pacific Northwest National Laboratory
Richland, Washington 99354

Summary

This study investigates the uncertainty of wave resource assessments due to sea ice in the nearshore region of Alaska using an innovative approach of combining remotely sensed data and a third-generation phase-averaged wave model. Modeling analysis focused on winter months, when high wave energy is present along with sea ice. This study includes recommendations to improve the accuracy of wave resource assessments and optimize marine and hydrokinetic device siting with consideration of sea-ice effects. Additional recommendations, based on preliminary sea-ice information in Cook Inlet, Alaska, are provided for a trajectory analysis of drifting sea ice and a collision risk assessment of sea ice and tidal turbines.

The outcome of this project will provide valuable information about the level of sea-ice impact on the accuracy of wave resource assessments in the Alaska nearshore region, and of sea-ice collision risk with MHK devices and ocean observation systems during winter months when sea ice is present.

Acknowledgments

The project is funded by the U.S. Department of Energy, Office of Energy Efficiency and Renewable Energy, Water Power Technologies Office under Contract DE-AC05-76RL01830 to Pacific Northwest National Laboratory.

Acronyms and Abbreviations

DOE	U.S. Department of Energy
FVCOM	Finite Volume Community Ocean Model
H_s	significant wave height
MHK	Marine and HydroKinetic
NDBC	National Data Buoy Center
PBE	Powering the Blue Economy
PWS	Prince William Sound
SWAN	Simulating WAves Nearshore

Contents

Figures

Table

1.0 Introduction

The Alaska coastal ocean, which is the largest Exclusive Economic Zone in the United States, has the largest wave and tidal energy resources in the nation [EPRI, 2011]. However, the presence of sea ice along the coast poses a great challenge to accurate wave resource assessments, marine and hydrokinetic (MHK) energy project siting, and deployment of ocean observation systems. Figure 1.1 shows extensive ice coverage in part of Alaska coast in January that has melted by April. Growing interest in Alaska's coastal ocean is validated by the area's designation as the nation's top tidal energy hotspot, boasting the nation's highest wave energy resource and great potential for Powering the Blue Economy (PBE) applications (e.g., powering ocean observation sensors and offshore aquaculture). However, most coastal areas in Alaska experience sea-ice coverage and extreme storms, especially during the winter months. To overcome this environmental barrier, it is important to understand and assess the sea-ice effect on wave resource assessments and its potential risk to MHK energy and ocean observation development.

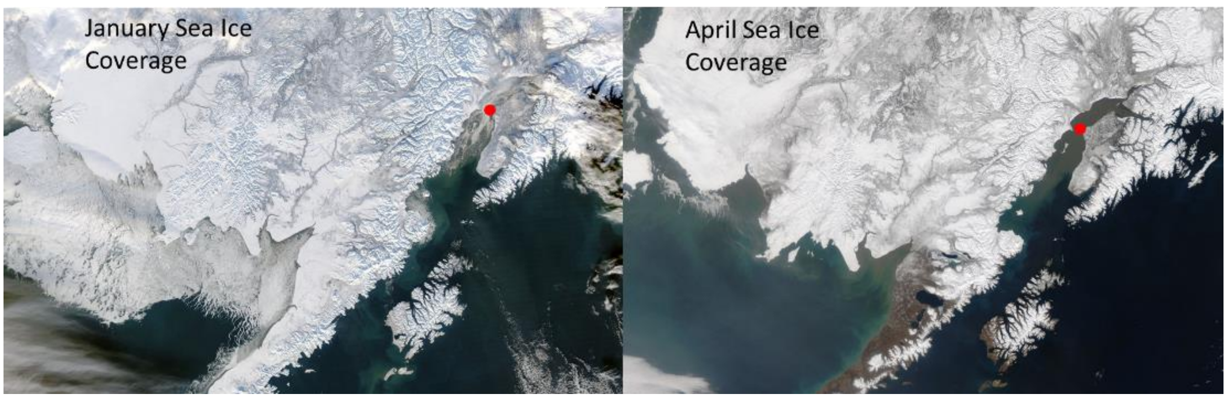

Figure 1.1. Sea-ice coverage in January (left) and April (right) in southeastern Bering Sea, Alaska Peninsula, south central Alaska, and Kodiak regions. The red dot denotes the tidal hotspot in Cook Inlet, Alaska, which is surrounded by ice in winter but free of ice in spring.

The most recent wave resource characterization and assessment in the Alaska region did not consider the effect of sea-ice coverage (Yang et al. 2019). The objective of this study is to evaluate the impacts of sea ice on wave resource assessments in the nearshore region of Alaska through a combination of satellite sea-ice data analysis and numerical simulations. The objective can be achieved through the following specific activities:

- compile and process satellite altimetry data in Alaska regions, analyze sea-ice coverage, and assess areas of potential impacts on MHK energy and ocean observation development
- conduct wave hindcast modeling along the Alaska coast with consideration of sea-ice coverage in the model domain (treated as land-cover) and compare the results with the existing hindcast modeling results to assess the uncertainty in wave resource, especially in the nearshore during winter months.

2.0 Methodology

The scope of the study is achieved through following three tasks:

1. Sea-ice characterization using satellite data.
2. Uncertainty analysis of Alaska wave hindcast due to sea ice.
3. Wave hindcast improvement with sea-ice addition.

2.1 Satellite Data of Sea Ice

Sea-ice coverage can be obtained from either visible wavelength or passive microwave satellite data. Passive microwave data has advantages over visible wavelength data in that it can be obtained regardless of cloud cover or daylight conditions. The analyses shown in this report used passive microwave data. Sea-ice concentration maps were obtained from data collected by the AMSR-2 instrument on JAXA's GCOM-W1 satellite (Spreen et al. 2008, Beitsch et al. 2014). The raw data were converted into sea-ice concentration maps using the ARTIST Sea Ice (ASI) algorithm (Beitsch et al. 2014). The maps provide daily coverage at 3.125 km resolution. The AMSR-2 data are available from August 2012 until the present. For sea-ice data before 2012, a 25 x 25 km daily passive microwave sea-ice concentration product is available from the National Snow and Ice Data Center.[1]

Table 2.1. Sea-ice data sets

Instrument	Spatial Resolution (km)	Temporal Resolution	Conditions	Availability
MODIS	1	~ 6 hours	daylight, clear skies	1999-present
AMSR2	3.125	daily	all weather, day or night	2012-present
SSMR/SSM/I	25	daily	all weather, day or night	1979-present

2.2 Alaska Regional Wave Hindcast Data

In a previous study, high-resolution wave hindcast was used to characterize the wave resource in the Alaskan nearshore region (Yang et al. 2019). The hindcast simulated the wave climate from 1979 to 2010 and 2017 in southern Alaska (Figure 2.). It used an unstructured, nested-grid modeling approach that incorporated WAVEWATCH III and a high-resolution Simulating WAves Nearshore (SWAN). However, the hindcast with SWAN version 41.01A did not consider the sea-ice effect. To determine the impact of sea ice on waves, this study compares hindcast data to in situ wave buoy measurements under different ice conditions. The hindcast data also provides open boundary conditions offshore to drive a new SWAN model with sea-ice capability to investigate the effect of sea ice on the wave climate in the nearshore areas.

[1] https://nsidc.org/data/g02202

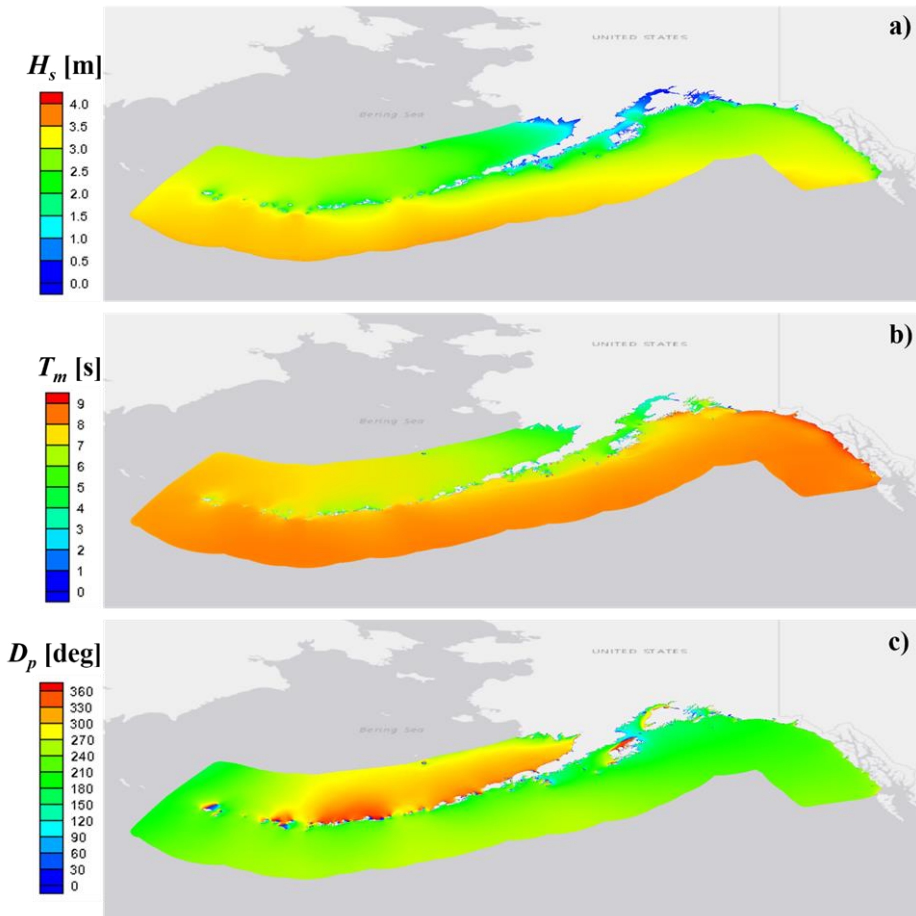

Figure 2.1 Yearly distributions of three wave bulk parameters in 2010: (a) significant wave height, (b) mean wave period, and (c) peak wave direction on the Alaska coast.

2.3 Wave Model with Added Sea-Ice Effect

The latest version (v41.31) of the SWAN model includes an implementation of the effects of sea ice on waves. The implementation describes the dissipation of wave energy as a polynomial dependent on wave frequency. The coefficients of the polynomial are an input to the model and vary with ice type. Currently, coefficients are available for ice floes 10 to 25 cm in diameter (Meylan et al. 2014) or for pancake and frazil ice (Rogers et al. 2018). The model user inputs the coefficients for the ice type in the study region and a grid of the ice concentration percentage. The analyses presented here for Alaska were conducted using the coefficients for 10 to 25 cm diameter floes and ice concentration percentages from the AMSR-2 3.125 km resolution data.

3.0 Results Analysis and Discussion

The following sections describe sea-ice analysis, existing wave hindcast error statistics, and an assessment of sea-ice effect.

3.1 Sea-Ice Coverage in Alaska

From 2001 to 2020, ice coverage surveys covered all of Alaska, with detailed examinations taking place around Prince William Sound (PWS) in the Gulf of Alaska on the south coast of Alaska. Ice coverage is ephemeral in some locations and persistent all winter in other locations. Average monthly mean sea-ice concentration maps show that ice coverage changes dramatically throughout the year (Figure 3.1). The north coast was found to have significant coastal ice from November until June, Cook Inlet was found to have significant ice concentrations from December to April, and PWS was found to have variable ice coverage from December to April. Further, ice coverage varied dramatically between years at some locations (Figure 3.2). Ice was consistently found on the north coast in March but was found to vary dramatically between years in Bristol Bay.

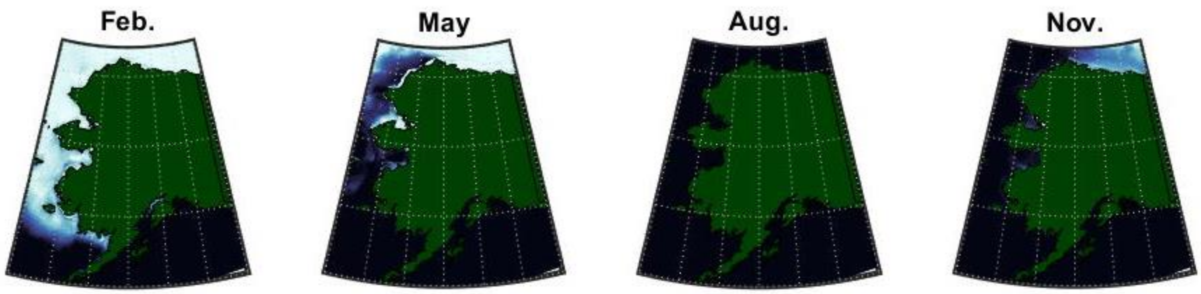

Figure 3.1. Intra-annual variability: average sea-ice concentration during February, May, August, and November of 2017.

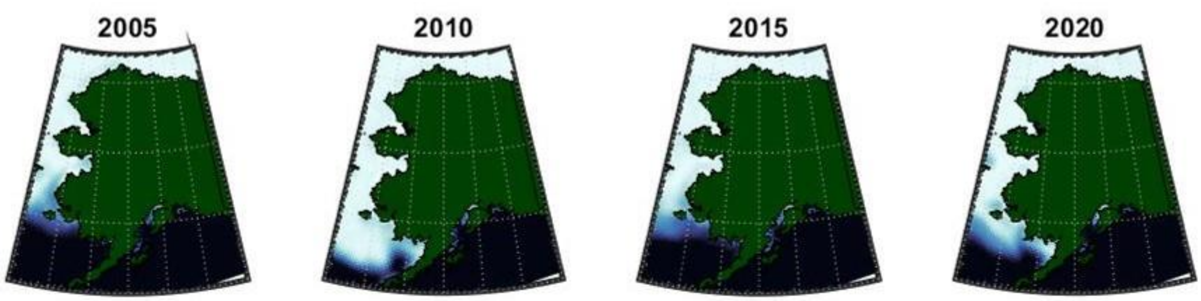

Figure 3.2. Interannual variability: average March sea-ice concentration.

Ice forms around the edges of PWS and occasionally across the Hinchinbrook Channel (Figure 3.3). Ice is not persistent all winter but changes daily.

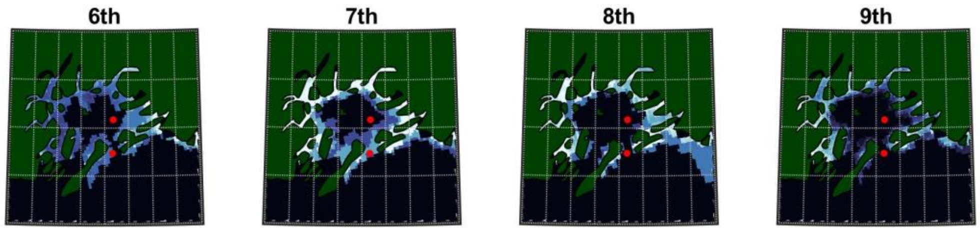

Figure 3.3. Sea-ice changes in PWS from December 6 through 9, 2017. National Data Buoy Center (NDBC) buoy locations are marked with red dots. Buoy 46060 is in PWS and buoy 46061 is just outside the PWS.

3.2 Effect of Sea Ice on Waves

It is known that sea ice affects waves, but the exact nature of wave energy dissipation by ice is a current topic of research. As sea ice begins to form on the ocean, it dampens out short surface waves (Sandven et al. 2006). Larger swell waves have enough energy to penetrate far into the ice pack until they encounter thick, multiyear ice that scatters wave energy (Dumont et al. 2011).

To evaluate the accuracy of the existing wave hindcast that did not consider the effect of sea ice, simulated significant wave height was compared to the observed data. Figure 3.4 shows that when sea ice was not considered, the model overestimates significant wave height, h_s, at Hinchinbrook Channel (buoy 46061) during late November and early December 2017. Figure 3.5 shows that the model also overestimates h_s inside of PWS (buoy 46060) during the same period, even though the wave heights are smaller. Sea-ice concentration data were examined to determine if the overestimation was due to ice dissipating the wave energy—a process not captured by the existing wave hindcast using SWAN model v41.01A.

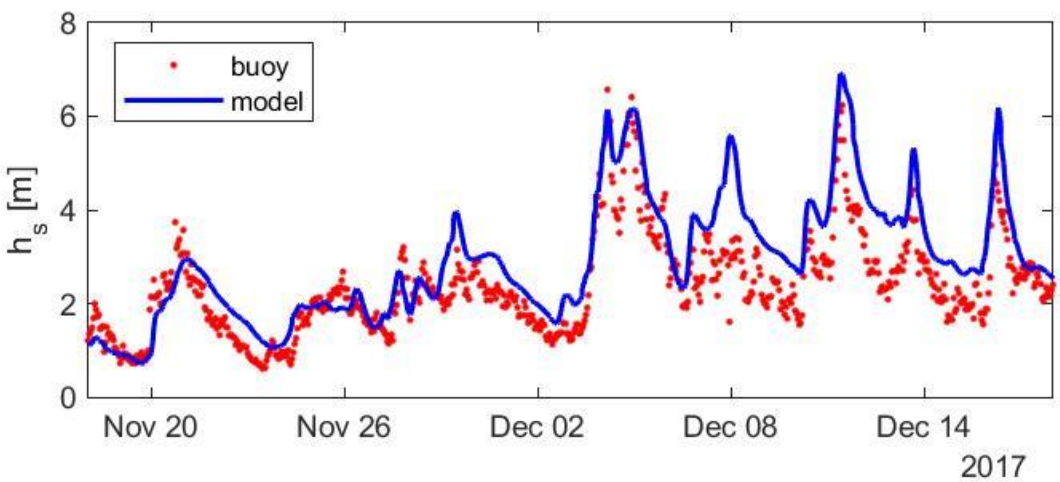

Figure 3.4. Time series comparisons of buoy and modeled significant wave height, h_s, at Hinchinbrook Channel (buoy 46061) during the winter of 2017.

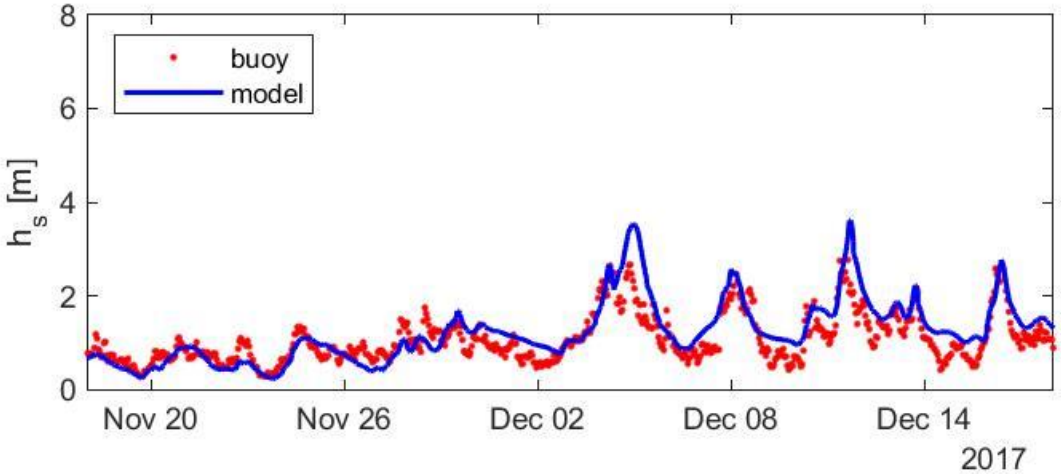

Figure 3.5. Time series comparisons of buoy and modeled significant wave height, h_s, inside PWS (buoy 46060) during the winter of 2017.

Satellite ice concentration data were averaged near buoy 46061 in 2017 and the significant wave height data were classified using the percentage of ice concentration at that location. When the ice concentration was less than 20 percent, the differences between the model and buoy h_s values were less than 0.5 m for all h_s conditions. When the ice concentration was greater than 20 percent, the differences were greater than 0.5 m for all h_s conditions. These results confirm that the sea ice is dissipating wave energy and the model is overestimating h_s when sea ice is present by not accounting for this process (Figure 3.6).

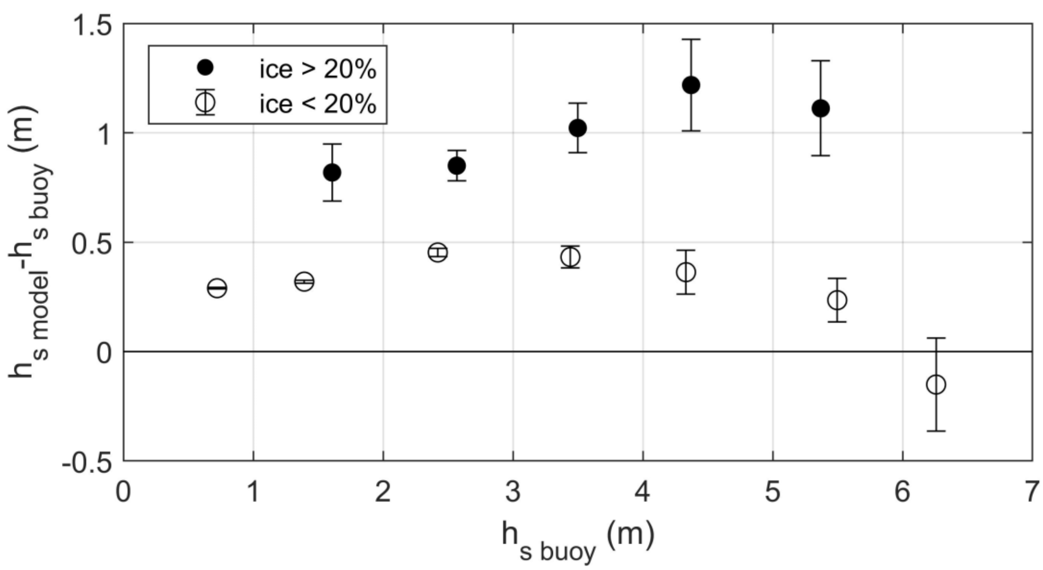

Figure 3.6. Difference between model and buoy h_s values at Hinchinbrook Channel during 2017 (buoy 46061) for ice coverage above and below 20 percent.

3.3 Modeling the Effects of Sea Ice on Waves

The latest version of the SWAN model (v41.31) with the sea-ice module, was used to study the effects of sea ice on waves in PWS. PWS has complex bathymetry with many islands and inlets

(Figure 3.7a). Waves coming from the south propagate through Hinchinbrook Channel into PWS where they are dissipated and become smaller at the NDBC buoy 46060 inside PWS than at NDBC buoy 46061 in the channel (Figure 3.7b). Ice concentration data measured by the AMSR-2 satellite instrument at 3.125 km resolution shows ice around the edges of PWS on December 7, 2017 (Figure 3.7c). The model was executed with and without ice on a 500 m structured grid with an open boundary condition of waves coming from the south. Model runs were conducted for significant wave heights of 1.5, 2.5, 3.5, 4.5, and 5.5 m at the open boundary. The model runs with sea ice show smaller significant wave heights than those without ice, which in turn improved the model accuracy. An example of this difference for 5.5 m incoming waves is shown in Figure 3.7d where the difference is large outside the channel where ice is located and inside PWS where the waves have been dampened by ice across the channel. These results show that running SWAN without including the effects of sea ice lead to overestimations of the significant wave heights.

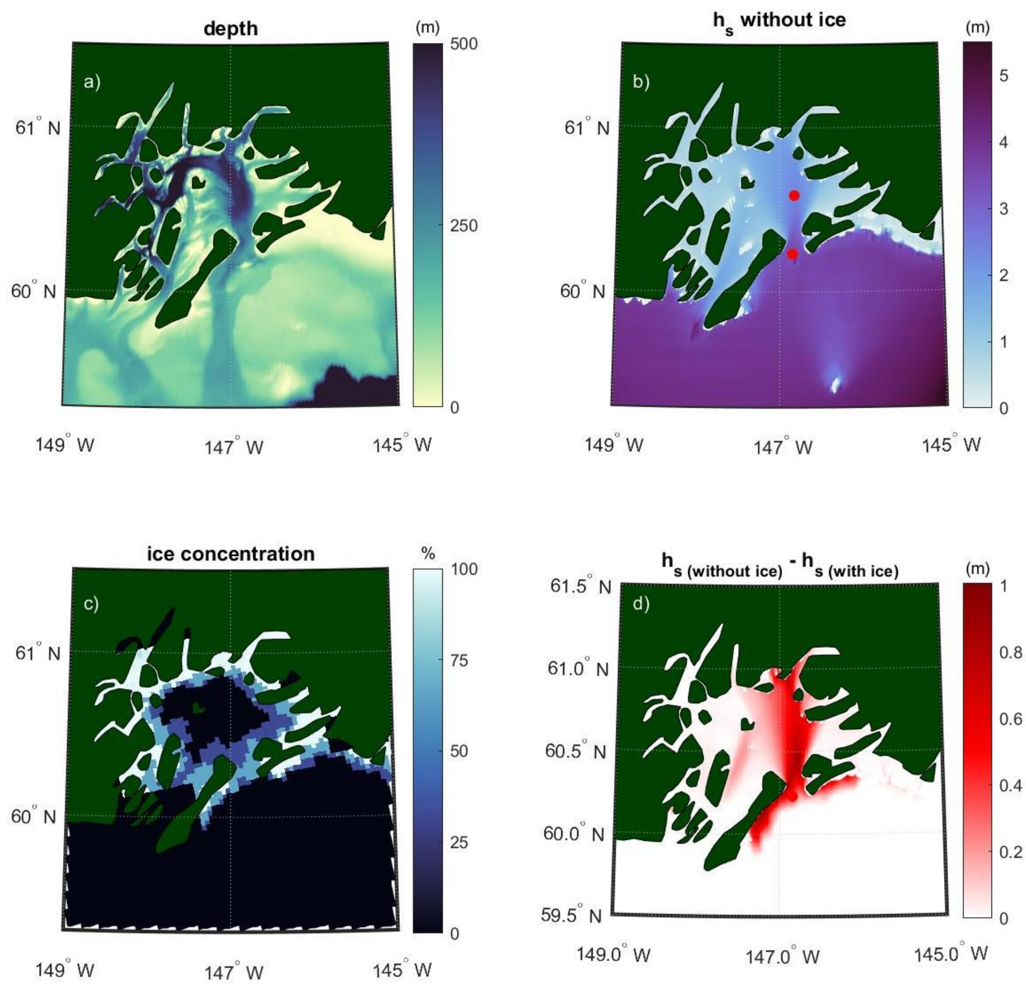

Figure 3.7. SWAN study of the effects of sea ice on waves. A) Bathymetry of PWS in Alaska. B) Simulated significant wave height driven by incoming waves of 5.5 m from the south. C) Sea-ice concentration map from AMSR-2 passive microwave data on December 7, 2017. D) Map of the difference between significant wave heights modeled without ice vs. with ice.

The level of the sea-ice effect on wave climate depends on the amount of sea ice present and the size of the incoming waves, which can be characterized by a set of sea-ice dissipation coefficients used in SWAN. A series of sensitivity model runs were carried out to evaluate the effect of the sea ice on wave climate for incoming waves with wave heights varying from 1.5 to 5.5 m. For simplicity, all the model runs were configured with a sea-ice coverage condition on December 7, 2017 (Figure 3.7c) and sea-ice coefficients for one type of ice. Figure 3.8 shows that the model errors were substantially reduced when the sea-ice effect was considered in the new SWAN model runs for the conditions where sea-ice coverage was greater than 20 percent. Clearly, the implementation of sea-ice effects in SWAN improves the accuracy of simulated significant wave heights when ice is present. Further model improvement can be achieved by better configuring the model coefficients for representing the sea-ice effect.

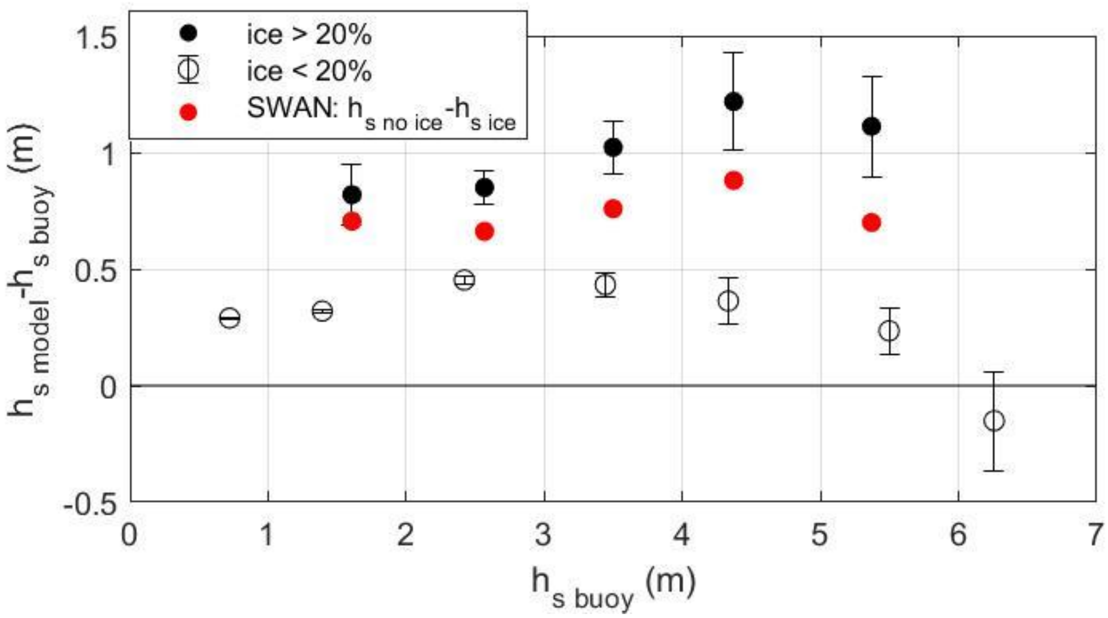

Figure 3.8. Difference between model and buoy h_s values at Hinchinbrook Channel during 2017 (buoy 46061) for ice coverage above and below 20 percent and that difference for the high ice coverage cases with the SWAN correction applied.

3.4 Drifting Sea ice in Cook Inlet

Cook Inlet is ranked as the top tidal stream energy site in U.S. coastal waters because of its strong tidal currents. However, Cook Inlet also experiences drifting sea ice (Figure 3.9) and extensive sea-ice coverage, especially in the upper inlet (Figure 3.10) during winter months of the year. The combination of strong tidal velocities in an area with drifting sea ice means that collisions may occur between the ice and offshore structures, especially tidal turbines in the water. While risk analysis of drifting sea ice on tidal turbines in Cook Inlet is beyond the scope of the study, Figure 3.9 and Figure 3.10 demonstrate the need of mapping areas prone to sea-ice collisions in Cook Inlet for tidal energy development.

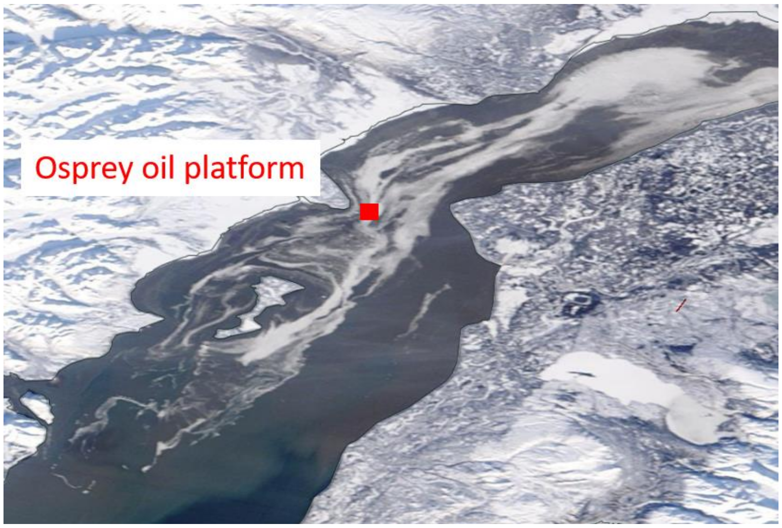

Figure 3.9. Drifting sea ice in Cook Inlet on (2/2/2017).

Figure 3.10. Pillars carve a path through the ice as the tide moves ice around in Cook Inlet (photo credit: U.S. Coast Guard).

4.0 Summary and Recommendations

A preliminary model study was conducted to investigate the effect of sea ice on wave climate near the Alaska coast using a combination of wave modeling, buoy measurements, and satellite data analysis. Key findings of the study include the following:

1. Buoy measurements in Hinchinbrook Channel show that large wave energy exists even in sea-ice coverage areas.
2. Correlations between the hindcast error and sea-ice coverage (seasonal trends) indicate the current hindcast overpredicts wave height in marginal ice zone of Alaska Coast.
3. The new version of SWAN, with sea-ice effect, improved hindcast accuracy, demonstrating the modeling capability of simulating sea ice and wave interaction in the Alaska coast and Arctic environment.
4. Extensive presence of drifting sea-ice in Cook Inlet, which indicates the need to consider sea-ice effect in MHK device siting in Cook Inlet and other high latitude coastal environments.

Recommendations for future research include the following:

1. Conduct sea-ice drifting and trajectory simulations in Cook Inlet using the Finite Volume Community Ocean Model (FVCOM) with input of satellite data and assess collision risk of drifting sea ice and tidal turbine farms in Cook Inlet. Identify optimal locations for tidal turbine farm deployment with consideration of sea-ice effect.
2. Extend high-resolution wave hindcast to northern Alaska and Arctic region and improve existing wave hindcast using the new SWAN model with sea-ice effect and satellite input to support remote coastal resilience. Refine resource assessment in the regions with sea-ice coverage and identify areas with a strong annual resource to support PBE.
3. Investigate the variations of wave resource with the extent of ice coverage and type of ice using both satellite and wave hindcast data and correlate wave resource change with sea ice characteristics.
4. Characterize ice type and its dampening effects on sea ice in the marginal ice zone to improve model accuracy in simulating sea ice and wave interactions. Ice type can be characterized using passive microwave data from the same instrument used to measure ice concentration percentage.
5. Undertake a comprehensive review of the current state of MHK devices to understand technology challenges and gaps. This is necessary because to harvest wave and tidal energy in ice environment, MHK devices must be designed to survive and operate either below the surface or at the surface while withstanding collisions with ice.

5.0 References

EPRI. Mapping and assessment of the United States ocean wave energy resource. In: EPRI 2011 technical report to U.S. Department of energy. Palo Alto, California: Electric Power Research Institute; 2011.

Yang Z, W Wu, T Wang, G Garcia Medina, and L Castrucci. 2019. High-Resolution Regional Wave Hindcast for the U.S. Alaska Coast. United States: DOI:10.2172/1579259, PNNL-29479. Pacific Northwest National Laboratory, Richland, Washington.

Rogers W, M Meylan, and A Kohout. 2018. Frequency distribution of dissipation of energy of ocean waves by sea ice using data from Wave Array 3 of the ONR “Sea State” field experiment. *NRL Report NRL/MR/7322-18-9801*.

Sandven S, OM Johannessen, and K Kloster. 2006. Sea ice monitoring by remote sensing. Encyclopedia of Analytical Chemistry: Applications, Theory and Instrumentation. John Wiley & Sons, Ltd.

Dumont D, A Kohout, and L Bertino. 2011. “A wave-based model for the marginal ice zone including a floe breaking parameterization.” *Journal of Geophysical Research: Oceans* 116.C4.

Meylan MH, LG Bennetts, and AL Kohout. 2014. “In situ measurements and analysis of ocean waves in the Antarctic marginal ice zone.” *Geophysical Research Letters* 41(14).

Spreen G, L Kaleschke, and G Heygster. 2008. “Sea ice remote sensing using AMSR-E 89-GHz channels.” *Journal of Geophysical Research: Oceans* 113 (C2).

Beitsch A, L Kaleschke, and S Kern. 2014. “Investigating high-resolution AMSR2 sea ice concentrations during the February 2013 fracture event in the Beaufort Sea.” *Remote Sensing* 6(5).

Nakata K, Ohshima KI, and Nihashi S. 2019. Estimation of thin-ice thickness and discrimination of ice type from AMSR-E passive microwave data. IEEE transactions on geoscience and remote sensing, 57(1).

PNNL- 30235

Pacific Northwest National Laboratory

902 Battelle Boulevard
P.O. Box 999
Richland, WA 99354
1-888-375-PNNL (7665)

www.pnnl.gov